TRANSITIONAL YIELDING APPROACH FOR SOILS UNDER GENERAL LOADING

By Yii-Wen Pan,[1] S. M. ASCE, and Sunirmal Banerjee,[2] M. ASCE

ABSTRACT: Within the framework of critical state soil mechanics concepts, a rate-independent constitutive model for soil response to complex, three-dimensional loading is proposed. For any loading excursion, the material response is assumed to be elastoplastic. The approach proposed permits description of continuous and transitional yielding of material by adopting a combination of isotropic and kinematic hardening law. The capability of the model to represent anisotropic hardening behavior of soils and soil behavior under cyclic loading is particularly emphasized. Predicted response of Kaolin samples is compared with experimental results from various types of laboratory tests, including true triaxial tests.

INTRODUCTION

The first rational basis for the synthesis of soil mechanics and isotropic hardening theories of plasticity was provided by Drucker, Gibson, and Henkel (9). The thrust of this work led to the development of the so-called "Cam-clay" concepts (18) for modeling the continuous yielding and volume change behavior of soils. And, since then, many refinements and improvements in the application of plasticity theories in geomechanical modeling have been proposed. Among the subsequent developments, including those that are direct derivatives of the Cam-clay model, some retain the original framework of isotropic hardening theory with associated flow rule (3,7,8,16,18,19,25), while others attempt to address more complex aspects of soil behavior by including kinematic hardening (13,17), and nonassociated flow rule (3,11).

Notwithstanding the great strides that have been made in plasticity modeling during the last two decades, some of the modified versions of the Cam-clay model (3,16,19) and a similar formulation called Cap model (2,20) have been most widely used. For the most part, this popularity is probably due to the mathematical simplicity of these formulations and of the parameter identification procedures consistent with the conventional laboratory tests. Nevertheless, these models, like many others, have considerable difficulty in predicting soil response for loading paths other than those from which model parameters are obtained. Secondly, these models are essentially limited to monotonic loading problems. Because of the underlying assumption of elastic behavior below the current yield surface, these models cannot account for the hysteresis effects due to stress reversals adequately, and do not have the ability to represent permanent deformations for stress reversals within the current yield sur-

[1]Asst. Prof., Natl. Chiao Tung Univ., Hsinchu, Taiwan; formerly, Grad. Student, Dept. of Civ. Engrg., Univ. of Washington, Seattle, WA 98195.

[2]Asst. Prof., Dept. of Civ. Engrg., Univ. of Washington, Seattle, WA 98195.

Note.—Discussion open until July 1, 1987. To extend the closing date one month, a written request must be filed with the ASCE Manager of Journals. The manuscript for this paper was submitted for review and possible publication on August 1, 1985. This paper is part of the *Journal of Engineering Mechanics*, Vol. 113, No. 2, February, 1987. ©ASCE, ISSN 0733-9399/87/0002-0153/$01.00. Paper No. 21222.

face. Furthermore, these models have been found to be lacking in their ability to account for soil response characteristics such as shear dilatancy, and initial and induced anisotropy. These are serious limitations, since in view of the preceding facts, such models should have limited utility for implementation in computational schemes for large-scale boundary value problems with real soils.

In a recent article (4), the writers proposed a transitional yielding approach to modeling unload-reload behavior of soils. This approach addresses the deficiency of the popular plasticity models in describing hysteresis effects by incorporating continuous changes in yield surfaces and plastic moduli during stress reversals. The possibilities of such an approach in representing the behavior of overconsolidated soils and the accumulation of permanent deformation due to unloading and reloading were demonstrated in that paper within the context of the modified Cam-clay formulations. In this paper, a similar approach is extended to a more complete model, which is mathematically simple yet accounts for any arbitrary three-dimensional anisotropic load-deformation response, including response to large stress reversals. The purpose of this paper is to present the theoretical formulations of the model, to show how the model parameters can be identified from simple tests and to examine the capabilities and accuracies of predictions.

Formulation of Theoretical Model

In the development that follows, any general three-dimensional loading history is considered to be composed of several individual stress paths. The material is assumed to be on the same stress path until a sudden reversal in the direction of stresses occurs. A new stress path is assumed to begin from the point of stress reversal. In order to account for realistic soil response to large stress reversals in a consistent manner, it has been hypothesized that a new set of yield surfaces begins to grow from the point of most recent stress reversal. The point of reversal on a stress trajectory can be easily defined and detected as the point at which the next increment of stress brings the stress state inside the current yield surface. As can be seen later, the definition of the point of stress reversal is crucial to this formulation.

Constitutive Relations.—The incremental approach to the elastoplastic hardening assumes that the total strain increment, $d\epsilon_{ij}$, due to a stress increment, $d\sigma_{ij}$, can be decomposed as

$$d\epsilon_{ij} = d\epsilon^e_{ij} + d\epsilon^p_{ij} \quad \ldots\ldots (1)$$

The elastic strain increments are easily related to the stress increments by

$$d\epsilon^e_{ij} = \frac{d\sigma_{ij}}{2G} - \frac{\mu}{E}\delta_{ij}d\sigma_{kk} \quad \ldots\ldots (2)$$

where G = shear modulus; E = Young's modulus; and μ = Poisson's ratio. The plastic strain increment can be related to the stress increment once the yield surface, the flow rule and the hardening modulus are all defined.

Yield Surface.—It is customary in all incremental theories of plasticity to represent the yield surface of an initially yielded material as

$$F(\sigma_{ij}, k) = 0 \quad \ldots\ldots (3)$$

in terms of its current stress state, σ_{ij}, which represents the components of the stress tensor) and some hardening parameter, k, which is dependent on the strain history of the material. For isotropic work hardening materials, such a surface described by the loading function, F represents the boundary between virgin or normally consolidated states and the overconsolidated states in the stress space. Conventionally, overconsolidated stress-strain behavior is assumed to be elastic; for most soils, this is an inadequate representation. In fact, experimental results show that plastic deformation takes place for stress states below the original or virgin yield surface and the behavior is still work-hardening plastic. Clearly, within the context of monotonically expanding yield surfaces, the stress-strain behavior of normally consolidated soils alone can be described. In order to remedy this defect and to extend the generality of the constitutive models, several formulations have proposed continuous degradation or contraction of the original yield surface during unloading (1,4,6). Even these models have limited versatility. There are yet other features such as anisotropy, both initial and induced, which have not been properly handled by these isotropic hardening models. Again, none of these models are quite suitable for general cyclic loading problems. Although reasonable simulations of these characteristics have been shown by models using multiple yield surfaces and kinematic hardening approach (12,13,17), these models have other limitations, which will be discussed later.

In order to formulate a more generalized model, it seems necessary to adopt an approach that cannot only describe both normally consolidated and overconsolidated soil behavior adequately, but also can provide a smooth transition between these two states. Hence, the current formulation utilizes a transitional approach which combines both isotropic and kinematic hardening. For loadings directed beyond the virgin yield surface, isotropic hardening is retained, while for loading excursions within the virgin yield surface a kinematic hardening rule is also assumed to apply. But when the material is reloaded back to virgin yielding again, the kinematic hardening characteristics associated with the stress history gradually fade away.

The virgin yield surface ($F = 0$) is assumed to have the mathematical form:

$$F(\sigma_{ij}, a_c) = 0 \quad \ldots\ldots (4)$$

For stress increments moving outward from this surface, the virgin yield surface may expand monotonically. But if the stress increment is directed inward from this surface, this is a point of stress reversal, the yield surface collapses back to a point. As further unloading occurs, the yield surface is allowed to expand and translate simultaneously. The rate of expansion and translation are assumed to be identical and the mathematical form of this yield surface is assumed to be same as the virgin yield surface. Consequently, the new yield surface satisfies

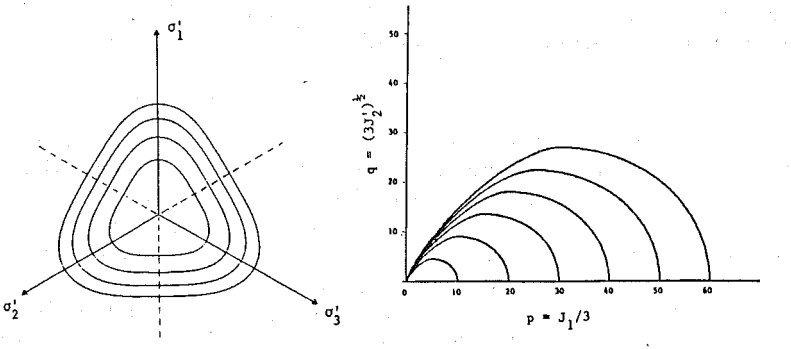

FIG. 1.—Typical Shapes of Yield Function in Principal Stress Space and in Triaxial (p,q) Plane

$$f(\sigma_{ij}^*, a) = 0 \quad \ldots\ldots (5)$$

where $a = sa_c$ = size of current yield surface so that the ratio of its size to that of the virgin yield surface; a_c is denoted by $s = a/a_c$, $0 \leq s \leq 1.0$; and $\sigma_{ij}^* = \sigma_{ij} - \alpha_{ij}$, with $\alpha_{ij} = (1 - s)\sigma_{ij}^R$ = a tensorial quantity that defines the amount of translation of the yield surface, and σ_{ij}^R = stress sensor at the point of most recent reversal.

A stress reversal condition occurs whenever the next stress increment, $\Delta\sigma_{ij}$, will bring the stress state inside the current yield surface described by Eq. 5. Under this condition

$$f(\sigma_{ij}^* + \Delta\sigma_{ij}, a) < 0 \quad \ldots\ldots (6)$$

In case any stress reversal occurs, the stress state σ_{ij} before the occurrence of stress reversal becomes the new σ_{ij}^R and the yield surface collapse to a zero size (or the ratio, s suddenly becomes zero at that point). Yield surface starts to expand and translate from then on following Eq. 5 again.

As the material is gradually loaded so that it gradually approaches virgin yielding, the size ratio, s, gradually approaches the value of unity. When $s = 1$, Eq. 5 becomes identical to the yield surface for virgin yielding ($f = F$).

The detailed derivation for the actual mathematical function used to represent the yield surface is provided in the Appendix I. The typical shapes of this function in the general stress space and the usual triaxial stress (p-q) plane are presented in Fig. 1 to illustrate that this functional form is capable of describing experimentally derived shapes (5,11).

Flow Rule.—The plastic strain increment $d\epsilon_{ij}^p$ resulting from any stress increment along any stress path is assumed to follow the flow rule, which may be expressed as

$$d\epsilon_{ij}^p = \frac{1}{H} n_{ij}^g (n_{mn}^f d\sigma_{mn}) \quad \ldots\ldots (7)$$

where n_{ij}^g = component of the unit normal vector on the plastic potential surface; n_{mn}^f = component of the unit normal vector on the current yield

surface $= (\partial f/\partial \sigma^*_{ij})/(\partial f/\partial \sigma^*_{mn} \cdot \partial f/\partial \sigma^*_{mn})^{1/2}$; $d\sigma_{mn}$ = component of stress increment; and H = hardening or plastic modulus, a scalar quantity. If the plastic potential surface and the yield surface are identical, i.e., an associated flow rule is assumed, Eq. 7 becomes

$$d\epsilon^p_{ij} = \frac{1}{H} n_{ij}(n_{mn} d\sigma_{mn}) \quad \ldots\ldots (8)$$

where $n^g_{ij} = n^f_{ij} = n_{ij}$. The hardening modulus for an initially yielded material can be evaluated from the consistency condition (i.e., $dF = 0$). In this study, the material response is assumed to be elastoplastic along any individual stress path, changing from purely elastic to virgin yielding gradually. This is controlled by the hardening modulus, which follows the interpolation rule given below.

Interpolation Rule.—Obviously, the hardening or plastic modulus defined in Eqs. 7 and 8 changes with the direction and the state of plastic deformation and its variation with the yield surface accounts for the directional stiffness of the material. It is assumed that the modulus takes an infinite value at the beginning of the stress reversal and gradually approaches its value on the virgin yield surface. Here, the variation of hardening modulus is assumed to obey the following rule:

$$H = \alpha \left[\frac{(1 - s^\gamma)(1 + \beta s^\gamma)}{s^r} \right] + H_{cd} \quad \ldots\ldots (9)$$

where H_{cd} = hardening modulus on the virgin yield surface; α = an arbitrarily chosen calibration factor; β,γ = material parameters; s = a size ratio previously defined; and H = the hardening modulus for the current stress state.

Derivation of Elastoplastic Matrix.—The elastic and the plastic stress-strain relations given by Eq. 2 and Eq. 8 can be written in the matrix form as

$$d\boldsymbol{\epsilon}^e = \mathbf{D}^{-1} d\boldsymbol{\sigma} \quad \ldots\ldots (10)$$

and

$$d\boldsymbol{\epsilon}^p = \frac{\frac{1}{H}\frac{\partial f}{\partial \boldsymbol{\sigma}^*}\left[\frac{\partial f}{\partial \boldsymbol{\sigma}^*} \cdot d\boldsymbol{\sigma}\right]}{\left[\left(\frac{\partial f}{\partial \boldsymbol{\sigma}^*}\right)^T \left(\frac{\partial f}{\partial \boldsymbol{\sigma}^*}\right)\right]} \quad \ldots\ldots (11)$$

where $\mathbf{D}$ = elastic stiffness matrix; and H = hardening modulus.

From Eq. 1, 10, and 11, it can be shown that (24)

$$d\boldsymbol{\sigma} = \left[\mathbf{D} - \frac{\mathbf{D}\left(\frac{\partial f}{\partial \boldsymbol{\sigma}^*}\right)\left(\frac{\partial f}{\partial \boldsymbol{\sigma}^*}\right)^T \mathbf{D}}{H\left(\frac{\partial f}{\partial \boldsymbol{\sigma}^*}\right)^T \left(\frac{\partial f}{\partial \boldsymbol{\sigma}^*}\right) + \left(\frac{\partial f}{\partial \boldsymbol{\sigma}^*}\right)^T \mathbf{D}\left(\frac{\partial f}{\partial \boldsymbol{\sigma}^*}\right)} \right] d\boldsymbol{\epsilon}$$

or $d\boldsymbol{\sigma} = \mathbf{D}^{ep} d\boldsymbol{\epsilon}$ $\ldots\ldots (12)$

Eq. 12 gives the required constitutive relations for the incremental loading. In order to obtain the elastoplastic matrix, $\mathbf{D}^{ep}$, the flow vectors which constitute the matrix, and the hardening modulus must be evaluated. Let J_1^*, J_2^*, J_3^* denote stress invariants and θ_0^* denote the Lode angle in terms of σ_{ij}^*. The flow vectors in the general stress space can be written as

$$\frac{\partial f}{\partial \sigma_{ij}^*} = \left(\frac{\partial f}{\partial J_1^*}\right)\frac{\partial J_1^*}{\partial \sigma_{ij}^*} + \left(\frac{\partial f}{\partial \sqrt{J_2'^*}}\right)\frac{\partial \sqrt{J_2'^*}}{\partial \sigma_{ij}^*} + \left(\frac{\partial f}{\partial M}\right)\left(\frac{\partial M}{\partial \theta_0^*}\right)\frac{\partial \theta_0^*}{\partial \sigma_{ij}^*} \quad \ldots\ldots (13)$$

$$\text{Since} \quad f = f(J_1^*, J_2'^*, M \text{ and } a) \quad \ldots\ldots (14)$$

where $M = M(\theta_0^*)$.

However

$$\frac{\partial \theta_0^*}{\partial \sigma_{ij}^*} = \frac{-\sqrt{3}}{2\cos 3\theta_0^*}\left[\frac{1}{(J_2'^*)^{3/2}}\cdot\frac{\partial J_3'^*}{\partial \sigma_{ij}^*} - \frac{3J_3'^*}{(J_2'^*)}\cdot\frac{\partial \sqrt{J_2'^*}}{\partial \sigma_{ij}^*}\right] \quad \ldots\ldots (15)$$

Hence, the flow vectors can be evaluated as

$$\frac{\partial f}{\partial \sigma_{ij}^*} = C_1\frac{\partial J_1^*}{\partial \sigma_{ij}^*} + C_2\frac{\partial \sqrt{J_2'^*}}{\partial \sigma_{ij}^*} + C_3\frac{\partial J_3'^*}{\partial \sigma_{ij}^*} \quad \ldots\ldots (16a)$$

$$\text{where} \quad C_1 = \frac{\partial f}{\partial J_1^*} \quad \ldots\ldots (16b)$$

$$C_2 = \left[\frac{\partial f}{\partial \sqrt{J_2'^*}} - \frac{\sin 3\theta_0^*}{\sqrt{J_2'^*}}\cdot Y\cdot\left(\frac{\partial f}{\partial M}\right)\right] \quad \ldots\ldots (16c)$$

$$C_3 = -\frac{\sqrt{3}}{2}\cdot\frac{1}{(J_2'^*)^{3/2}}\cdot Y\cdot\left(\frac{\partial f}{\partial M}\right) \quad \ldots\ldots (16d)$$

$$\text{and} \quad Y = -\frac{1}{2}(1 - B^2)M^3(B\cdot M_c)^{-2} \quad \ldots\ldots (16e)$$

Eq. 16*e* is derived from the definition of $M = M(\theta_0)$ given in Appendix I. The quantities $\partial f/\partial J_1^*$, $\partial f/\partial \sqrt{J_2'^*}$, and $\partial f/\partial M$ can be easily computed from the definition of the yield function, f.

The hardening modulus, H_{cd} for virgin yielding state can be as shown in Appendix II as

$$H_{cd} = \frac{\dfrac{-a_c}{(\lambda_c - \kappa_u)}\left(\dfrac{\partial F}{\partial a_c}\right)(1+e)\dfrac{\partial F}{\partial \sigma_{kk}}}{\left(\dfrac{\partial F}{\partial \boldsymbol{\sigma}}\right)^T\left(\dfrac{\partial F}{\partial \boldsymbol{\sigma}}\right)} \quad \ldots\ldots (17)$$

in which a_c = mean normal stress at critical state; λ_c, κ_u = critical state parameters for virgin compression and swelling, respectively; and e = void ratio of soil.

Evaluation of Model Parameters.—It is clear from the preceding section that the parameters needed to characterize a particular soil are:

1. e_1 = reference soil ratio of the soil at unit mean stress.
2. λ_c = slope of the hydrostatic loading (compression) curve in e-ln p space.
3. κ_u = initial slope of the hydrostatic unloading (extension) curve in e-ln p space.
4. μ = Poisson's ratio.
5. M_c = stress ratio at critical state in compression = $6 \sin \phi_{max}/3 - \sin \phi_{max}$, in terms of maximum friction angle ϕ_{max}.
6. B = strength anisotropy factor; given by the ratio M_e/M_c in which M_e = stress ratio at critical state in extension = $6 \sin \phi_{max}/3 + \sin \phi_{max}$ in terms of maximum friction angle ϕ_{max}.
7. ω = factor defining the shape of yield surface on the wet side (in the terminology of critical state soil mechanics, ω is equivalent to $[(p_c - a_c)/a_c]$.
8. d = calibration constant defining the shape of yield surface on the dry side.
9. β and γ = calibration constants for interpolation of hardening modulus.

Realizing that the set of parameters listed above must be evaluated from suitable experimental data, particular emphasis was placed on requiring that the parameter identification procedures be based on standard triaxial laboratory tests. The first six of the parameters listed are common to all "Cam-clay" type of models and can be easily evaluated. The parameters, λ_c and κ_u can be evaluated from isotropic consolidation test with at least one unload-reload cycle. M_c and B can be evaluated from triaxial compression and extension tests on normally consolidated samples and the Poisson's ratio, μ from the initial slope of the triaxial compression or extension data.

The remaining parameters germane to the proposed model would require somewhat sophisticated testing. The material constants ω, and d defining the shape of the yield surface on the wet and dry side of critical will require constant stress path drained triaxial tests on a number of samples at different overconsolidation ratio values. And, the hardening modulus interpolation parameters, β and γ need to be calibrated against reloading data from isotropic consolidation tests and against triaxial cyclic stress-strain data on a number of overconsolidated samples.

Examples and Verification

The proposed approach has been applied to several different types of common laboratory tests for soils. First, the theoretical response of an example soil under both static and cyclic laboratory tests were numerically simulated. The whole idea behind these simulations was to demonstrate the capabilities of this model. The accuracies of model prediction were also verified by a series of comparisons between experimental observations of stress-strain or pore pressure responses furnished in the

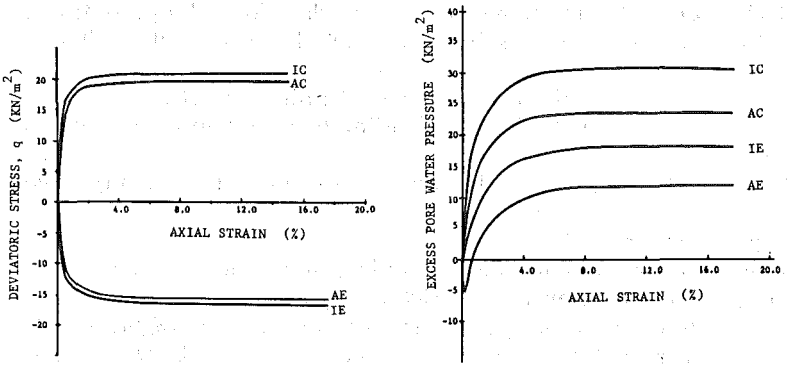

FIG. 2.—Theoretical Deviatoric Stress and Pore Pressure Response in Undrained Triaxial Compression (ACU and ICU) and Extension (AEU and IEU) Tests

literature and those predicted by the model. These results are discussed in this section.

The effect of isotropic and anisotropic (K_o) consolidation on the undrained shear response of soils is shown in Fig 2. This figure presents the numerically preicted results of CU triaxial compression (IC and AC) and extension (IE and AE) tests on a normally consolidated specimen. Figs. 2(*a–b*) show the variation of deviatoric stresses, and excess pore pressures, respectively, against axial strain. Theoretical results of cyclic undrained simple shear tests on an isotropically consolidated specimen are presented in Fig. 3 in terms of shear stress and excess pore pressure buildup, respectively, against shear strain. Simulated responses of the soil under drained simple shear conditions are shown in terms of shear stress and volumetric strain versus shear strain in Fig. 4.

The model parameters used for the soil specimen are $\lambda_c = 0.24$, $\kappa_u = 0.04$, $e_1 = 2.79$, $\mu = 0.15$, $\gamma = 4$, $\beta = 60$, $\omega = 1.25$, $d = 10$, $B = 0.8$ and $M_c = 0.85$. For all the cases the initial isotropic confining pressure (or the vertical pressure for K_o-consolidation cases) was maintained to be 50 kN/m^2. These examples adequately display the capability of the approach to model the differences in undrained strength in static triaxial compression and extension, the hysterisis effects and generation of porepressures or accumulation permanent volumetric strains in cyclic simple shear tests.

The experimental data reported by several authors (15,19,22,23) on Kaolin samples were used in this study for comparison with predicted responses. The data selected include undrained triaxial compression and extension test results for both normally and overconsolidated specimens, undrained triaxial stress path data for monotonic and cyclic tests, and results of cubic triaxial drained tests performed at constant mean effective stress.

Fig. 5 shows the comparison between predicted deviatoric stress and excess pore pressure responses and the corresponding measured responses (15) for a specimen at OCR = 1.0, and 2.3 subjected to undrained triaxial compression and extension. Except for the pore pressure

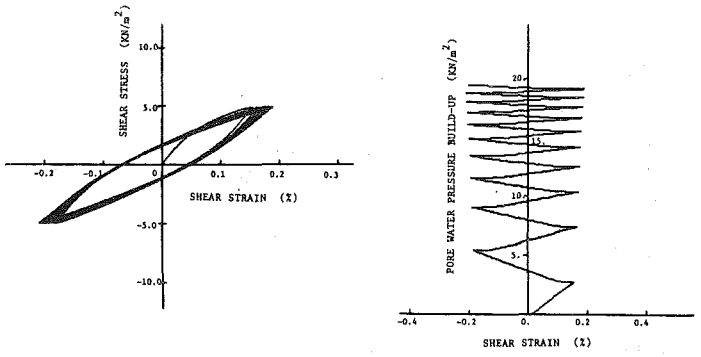

FIG. 3.—Theoretical Results of Undrained Cyclic Simple Shear Tests

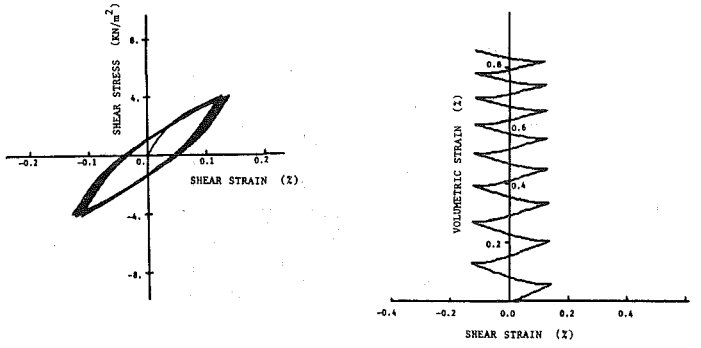

FIG. 4.—Theoretical Results of Drained Cyclic Simple Shear Tests

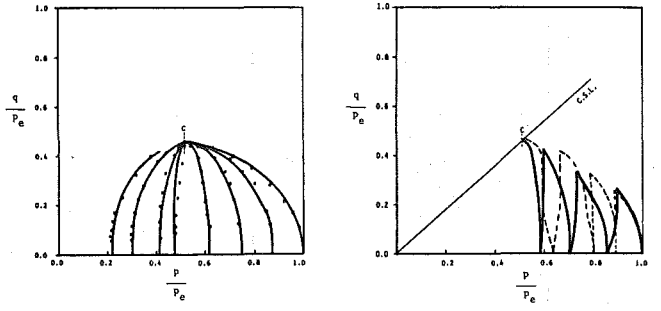

FIG. 5.—Comparison of Experimental (15) and Predicted Responses in Undrained Triaxial Tests

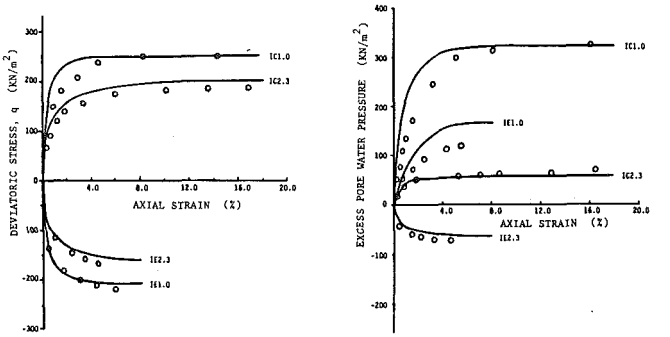

FIG. 6.—Comparison of Measured (23) and Predicted Undrained Stress Paths for Static and Cyclic Triaxial Tests

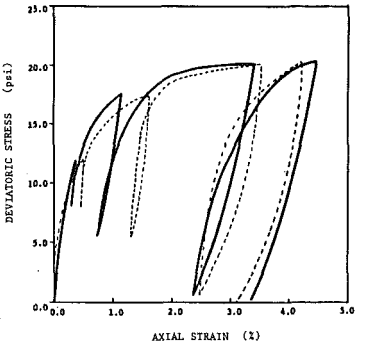

FIG. 7.—Comparison of Experimental (19) and Theoretical Stress-Strain Responses in Cyclic Undrained Triaxial Test

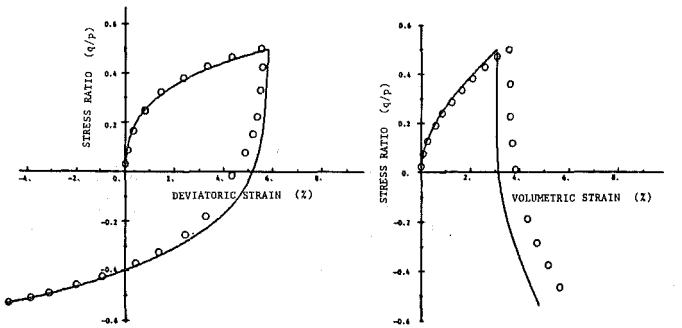

FIG. 8.—Comparison of Predicted and Measured (22) Responses in Drained (p = Constant) Cubical Triaxial Test

response of the normally consolidated specimen during extension, the agreement with computed results is remarkable. Wroth and Loudon (23) provided experimental plots of normalized undrained stress paths for monotonic loading on Kaolin samples at various OCR values and for cyclic loading on normally consolidated samples. Fig. 6 shows how these plots compare with their theoretical counterparts. In this figure the solid lines denote the predicted paths and the point c represents the critical state. It can be seen that the results of the static tests compared significantly better than those of the cyclic test for some reason. Roscoe and Burland's (19) data from cycled undrained triaxial tests on a normally consolidated sample also show good agreement with the predicted results, which are shown in Fig. 7 by the solid lines. In the final example chosen for verification, the results obtained by Wood (14) from true triaxial tests on Kaolin samples are shown to match very well with the predictions in Fig. 8. This test was performed at constant mean stress, p by keeping one of the principal stresses constant and by gradually increasing and reducing the other two principal stresses by equal amounts under drained condition. The direction of the stress path was reversed after reaching a predetermined state. It can be noted that similar deviatoric and volumetric deformation characteristics were reported by Namy (14) for drained constant p-tests. A particularly encouraging feature of the predictions is the evidence of volume decrease even during the early part of stress reversal.

It is worth mentioning that in making prediction of the results selected for verifications, the model parameters did not require any significant alteration. Essentially, among the parametric values used for the example cases described above, only γ, β and M_c were slightly adjusted. The actual values used are: $\gamma = 5$, $\beta = 0$, $M_c = 0.82$ for Fig. 5; $\gamma = 4$, $\beta = 20$, $M_c = 0.9$ for Figs. 6 and 7; and $\gamma = 4$, $\beta = 0$, $M_c = 0.85$ for Fig. 8. This is particularly remarkable in view of the fact that the results were selected from different sources.

Summary and Conclusions

An incremental elastoplastic constitutive model for soils under general loading conditions has been proposed. The approach proposed herein is based on the concept of transitional yielding behavior and allows gradual change from elastic to inelastic behavior during both loading and unloading. An associated flow rule and a combined isotropic and kinematic hardening law was adopted for this model. While an isotropic hardening law applies adequately for virgin yielding of soils, a combined isotropic and kinematic hardening is needed for describing the behavior of preconsolidated material. The scheme adopted in this study for the growth of yield surfaces provides an alternative to the nested yield surface modeling (12,13,17). Contrary to the models using nested yield surfaces in which the location of all the yield surfaces during the process of loading needs to be traced and recalled, and a large number of nesting surfaces required to insure good results, the proposed model only requires a size ratio, s. As a result, this model may be much more efficient for application to actual boundary value problems.

The capabilities and accuracies of the model predictions have been demonstrated by analyzing a number of cases and comparing with experimental results from literature sources. It has been particularly shown that the model extends the application of critical state concepts to cyclic loading and anisotropic material behavior. The dilatant and strain-softening features of material behavior are also incorporated. Since majority of the material constants are essentially common to those in "Cam-clay" models, these are relatively easily evaluated; others are determined by fitting triaxial stress paths.

Evidently, the incremental constitutive relations proposed herein only apply for rate-insensitive, path-dependent material behavior so that phenomena such as creep or stress relaxation are not covered. However, in many complex practical problems in geotechnical engineering it may be possible to obtain a good estimate of behavior without including rate effects. In such circumstances, the proposed scheme has good potential for applications.

Appendix I.—Derivation of Yield Function in General Stress Space

In the general stress space the yield function has the form

$$F = F(J_1, \sqrt{J_2'}, \theta_0, a_c) \quad (18)$$

in which $\theta_0 = 1/3 \sin^{-1} [3\sqrt{3}/2(J_3'/J_2'^{3/2})]$; J_1 = first invariant of the stress tensor; J_2' = second invariant of the devatoric stress tensor; J_3' = third invariant of the deviatoric stress tensor; $S_{ij} = \sigma_{ij} - (1/3)\sigma_{kk}\delta_{ij}$ = deviatoric stress; σ_{ij} = stress tensor; δ_{ij} = Kronecker delta; and a_c = hardening parameter.

The yield function may also be expressed as a function of J_1, J_2', M, and a_c, with M = the stress ratio at the critical state. In order to take into account anisotropy, M is considered to be varying with the orientation of the stress path in the general stress space. In other words, M is assumed to be a function of θ_0. The actual functional form, $M = M(\theta_0)$ was obtained by mapping a quarter of an ellipse on one-sixth of the π-plane as

$$M = M(\theta_0) = \frac{BM_c}{\left[B^2 \cos^2\left(1.5\theta_0 + \frac{\pi}{4}\right) + \sin^2\left(1.5\theta_0 + \frac{\pi}{4}\right)\right]^{1/2}} \quad (19)$$

where $M = M_c$ when $\theta_0 = -\pi/6$ (triaxial compression test); $M = BM_c$ when $\theta_0 = \pi/6$ (triaxial extension test); and M_c, and B = material parameters.

Two different functions were selected for representing the segments of the yield surface on the wet and dry sides of critical. The stress ratio, which is given by $\eta = q/p$ where $q = \sqrt{3J_2'}$ = deviatoric stress and $p = J_1/3$ = mean normal stress, defines these two regions. The dry of critical state corresponds to $\eta > M$, while $\eta \leq M$ corresponds to the wet of critical state. In addition to satisfying continuity at $\eta = M$, the chosen yield functions are required to meet the following conditions: (1) @ $p =$

0; $q = 0$, $\partial F/\partial p < 0$, $\partial F/\partial q = 0$; (2) @ $p = a_c$; $q = Ma_c$, $\partial F/\partial p = 0$; $\partial F/\partial q > 0$, with a_c = the mean normal stress at critical state; and (3) @ $p = p_c$; $q = 0$, $\partial F/\partial p > 0$, $\partial F/\partial q = 0$, with p_c = the mean normal stress when $\eta = 0$.

Yield Function—Wet of Critical ($\eta \leq M$).—Since it has been seen that the modified Cam-clay type of surface works well for soils wetter than critical, a more general form of elliptical yield function was selected for this study. On the p-q plane, it can be written as

$$F = F_w = M^2(p - a_c)^2 + \omega^2 q^2 - \omega^2 M^2 a_c^2 = 0 \quad \ldots\ldots\ldots\ldots\ldots\ldots\ldots\ldots \quad (20)$$

where M = stress ratio at critical state defined by Eq. 19; a_c = mean normal stress at critical state; and ω = a material parameter defining the shape of the ellipse. The Eq. 20 can also be written in terms of the stress invariants as

$$F = F_w = M^2\left(\frac{J_1}{3} - a_c\right)^2 + 3\omega^2 J_2' - \omega^2 M^2 a_c^2 = 0 \quad \ldots\ldots\ldots\ldots\ldots\ldots\ldots\ldots \quad (21)$$

It should be pointed out that this yield surface is similar to the movable surface in the cap model (2,20). It can also be shown that when $B = 1.0$ (i.e., $M = M_c$ = constant) and $\omega = 1.0$, the yield surface adopted here becomes identical with its counterpart for the modified Cam-clay.

Yield Function—Dry of Critical ($\eta > M$).—For soils in dry states, an elliptical description of the yield surface is not particularly suitable. A more general yield function was, therefore, adopted for the dry side in terms of p, q as

$$F = F_d = (d - 1)p^d + \left(\frac{q}{M}\right)^d - d \cdot p^{(d-1)} \cdot a_c \quad \ldots\ldots\ldots\ldots\ldots\ldots\ldots\ldots \quad (22)$$

where d = a material calibration constant for the shape of the yield surface on the dry side. Again, Eq. 22 can be written in terms of the invariants as

$$F = F_d = (d - 1)\left(\frac{J_1}{3}\right)^d + \left(\frac{\sqrt{3J_2'}}{M}\right)^d - d\left(\frac{J_1}{3}\right)^{d-1} \cdot a_c = 0 \quad \ldots\ldots\ldots\ldots\ldots\ldots \quad (23)$$

It can be shown that when $B = 1.0$ (i.e., $M = M_c$ = constant and $d = 2$, the modified Cam-clay yield surface is traced. For larger values of d, the yield surface becomes flatter and flatter.

These two yield function together satisfy the three conditions prescribed earlier.

Appendix II.—Derivation of Hardening Modulus, H_{cd}

From the general expression for the yield surface $F = F(\boldsymbol{\sigma}, k)$ where k = hardening parameter. Consistency condition requires

$$dF = \left(\frac{\partial F}{\partial \boldsymbol{\sigma}}\right) \mathbf{d}\boldsymbol{\sigma} + \left(\frac{\partial F}{\partial k}\right) dk = 0 \quad \ldots\ldots\ldots\ldots\ldots\ldots\ldots\ldots\ldots\ldots \quad (24)$$

Also, from the flow rule

$$d\boldsymbol{\epsilon}^p = \frac{\left(\frac{\partial F}{\partial \boldsymbol{\sigma}}\right)\left[\left(\frac{\partial F}{\partial \boldsymbol{\sigma}}\right)^T \mathbf{d}\boldsymbol{\sigma}\right]}{H\left[\left(\frac{\partial F}{\partial \boldsymbol{\sigma}}\right)^T \frac{\partial F}{\partial \boldsymbol{\sigma}}\right]} \quad \ldots\ldots (25)$$

For any strain-hardening relationship, the change in k can be expected as

$$dk = \mathbf{Z}^T d\boldsymbol{\epsilon}^p \quad \text{where} \quad \mathbf{Z}^T = \text{a weighting matrix} \quad \ldots\ldots (26)$$

Hence from Eqs. 24–26 one obtains

$$\left(\frac{\partial F}{\partial \boldsymbol{\sigma}}\right)^T \mathbf{d}\boldsymbol{\sigma} + \left(\frac{\partial F}{\partial k}\right)\left[\frac{\mathbf{Z}^T\left(\frac{\partial F}{\partial \boldsymbol{\sigma}}\right)\left\{\left(\frac{\partial F}{\partial \boldsymbol{\sigma}}\right)^T \mathbf{d}\boldsymbol{\sigma}\right\}}{H\left(\frac{\partial F}{\partial \boldsymbol{\sigma}}\right)^T\left(\frac{\partial F}{\partial \boldsymbol{\sigma}}\right)}\right] = 0 \quad \ldots\ldots (27)$$

In other words, the hardening modulus is given by

$$H = -\frac{\left(\frac{\partial F}{\partial k}\right)\mathbf{Z}^T\left(\frac{\partial F}{\partial \boldsymbol{\sigma}}\right)}{\left(\frac{\partial F}{\mathbf{a}\boldsymbol{\sigma}}\right)^T\left(\frac{\partial F}{\partial \boldsymbol{\sigma}}\right)} \quad \ldots\ldots (28)$$

In this formulation, the weighting matrix, $\mathbf{Z}$ is taken as

$$\mathbf{Z} = \begin{bmatrix} 1+e \\ 1+e \\ 1+e \\ 0 \\ 0 \\ 0 \end{bmatrix} \quad \text{where} \quad e = \text{current void ratio} \quad \ldots\ldots (29)$$

so that the irrecoverable void ratio change is equal to the change in the hardening parameter, dk, i.e.

$$dk = de^p = (1+e)d\epsilon^p_{kk} \quad \ldots\ldots (30)$$

Again, from the consolidation relationship the mean normal stress at virgin yielding, p_c is given by

$$p_c = p_1 \exp\left(\frac{e^p}{\lambda_c - \kappa_u}\right) \quad \ldots\ldots (31)$$

where p_1 = reference mean normal stress = unit stress; and e^p = irrecoverable void ratio change due to change in stress from p_1 to p_c. Noting that p_c can also be written as

$$p_c = (1+\omega)a_c \quad \ldots\ldots (32)$$

the terms ω and a_c are defined in Appendix I. The quantity $(\partial F/\partial k)$ becomes

$$\frac{\partial F}{\partial k} = \left(\frac{\partial F}{\partial a_c}\right)\left(\frac{\partial a_c}{\partial p_c}\right)\left(\frac{\partial p_c}{\partial e^p}\right) \quad \text{(33a)}$$

$$\frac{\partial F}{\partial k} = \frac{p_c}{1+\omega}\frac{\left(\frac{\partial F}{\partial a_c}\right)}{(\lambda_c - \kappa_u)} \quad \text{(33b)}$$

$$\frac{\partial F}{\partial k} = \frac{a_c}{\lambda_c - \kappa_u}\left(\frac{\partial F}{\partial a_c}\right) \quad \text{(33c)}$$

The hardening modulus H_{cd} during virgin yielding can therefore be written in the form

$$H_{cd} = -\frac{\left(\frac{a_c}{\lambda_c - \kappa_u}\right)\left(\frac{\partial F}{\partial a_c}\right)(1+e)\frac{\partial F}{\partial \sigma_{kk}}}{\left(\frac{\partial F}{\partial \boldsymbol{\sigma}}\right)^T\left(\frac{\partial F}{\partial \boldsymbol{\sigma}}\right)} \quad \text{(34)}$$

Appendix III.—References

1. Amerasinghe, S. F., and Kraft, L. M. (1983). "Application of A Cam-Clay Model to Overconsolidated Clay." *Int. J. Num. Analyt. Methods Geomech.*, 7, 173–186.
2. Baladi, G. Y., and Rohani, B. (1979). "An Elastic-plastic Model for Saturated Sand Subjected to Monotonic and/or Cyclic Loadings." *Proc. 3rd Int. Conf. on Num. Method in Geomech.*, 1, 389–404.
3. Banerjee, P. K., and Stipho, A. S. (1978). "Associated and Non-Associated Constitutive Relations for Undrained Behavior of Isotropic Soft Clays." *Int. J. Num. Analyt. Methods in Geomech.*, 2, 35–56.
4. Banerjee, S., and Pan, Y. W. (1986). "A Transitional Yielding Approach for Modeling Clay Material Behavior." *J. Geotech. Engrg.*, ASCE, 112(12), 170–186.
5. Bishop, A. W. (1971). "Shear Strength Parameters for Undisturbed and Remoulded Soil Specimens." *Proc. Roscoe Mem. Symp. on Stress-Strain Behavior of Soils*, Parry, Ed., 3–58.
6. Carter, J. P., Booker, J. R., and Wroth, C. P. (1982). "A Critical State Soil Model for Cyclic Loading." Chapter 9, *Soil Mech.—Transient and Cyclic Loads, Constitutive Relations and Numerical Treatment*, Pande and Zienkiewicz, Eds., 219–252.
7. Dafalias, Y. F., and Herrmann, L. R. (1980). "A Bounding Surface Soil Plasticity Model." *Int. Symp. on Soils under Cyclic and Transient Loading*, Swansea, U.K.
8. Desai, C. S., and Faruque, M. O. (1984). "Constitutive Models for (Geological) Materials." *J. Engrg. Mech.*, 110(9), 1391–1408.
9. Drucker, D. C., Gibson, R. E., and Henkel, D. J. (1957). "Soil Mechanics and Work Hardening Theories of Plasticity." *Transactions*, ASCE, 122, 338–346.
10. Hardin, B. O. (1978). "The Nature of Stress-strain Behavior for Soils." *Proc.*, ASCE Geotech. Engrg. Div. Specialty Conf., 1, Pasadena, Calif., 3–90.
11. Lade, P. V., and Duncan, J. M. (1975). "Elastoplastic Stress-Strain Theory for Cohesionless Soil." *J. Geotech. Engrg. Div.*, ASCE, 101(10), 1037–1053.
12. Mroz, Z. (1967). "On the Description of Anisotropic Work-Hardening." *J. Mech. Phys. Solids*, 15, 163–175.
13. Mroz, Z., Norris, V. A., and Zienkiewicz, O. C. (1979). "Application of An Anisotropic Hardening Model in the Analysis of Elasto-Plastic Deformation of Soils." *Geotechnique*, 29, 1–34.

14. Namy, D. (1970). "An Investigation of Certain Aspects of Stress-strain Relationships of Clay Soils," thesis presented to Cornell University, at Ithaca, N.Y., in partial fulfillment of the requirements for the degree of Doctor of Philosophy.
15. Parry, R. H. G., and Nadarajah, V. (1973). "Observations on Laboratory Prepared, Lightly Overconsolidated Specimens of Kaolin." *Geotechnique*, 24(3), 345–358.
16. Pender, M. J. (1978). "A Model for the Behavior of Overconsolidated Soil." *Geotechnique*, 28(1), 1–25.
17. Prevost, J. H. (1978). "Anisotropic Undrained Stress-strain Behavior of Clays." *J. Geotech. Engrg. Div.*, ASCE, 104(8), 1075–1090.
18. Roscoe, K. H., Schofield, M. A., and Wroth, C. P. (1958). "On the Yielding of Soils." *Geotechnique*, 8(1), 22–53.
19. Roscoe, K. H., and Burland, J. B. (1968). "On the Generalized Stress-strain Behavior of 'Wet' Clay." *Engineering Plasticity*, Heyman and Leckie, Ed., Cambridge University Press, Cambridge, U.K., 535–609.
20. Sandler, I. S., Dimaggio, F. L., and Baladi, G. Y. (1976). "Generalized Cap Model for Geological Materials." *J. Geotech. Engrg. Div.*, ASCE, 102(7), 683–699.
21. Schofield, A. N., and Wroth, C. P. (1968). *Critical State Soil Mechanics*, McGraw-Hill, London, U.K.
22. Wood, D. M. (1975). "Explorations of Principal Stress Space with Kaolin in a True Triaxial Apparatus." *Geotechnique*, 25(4), 783–797.
23. Wroth, C. P., and Loudon, P. A. (1967). "The Correlation of Strains within a Family of Triaxial Tests on Overconsolidated Samples of Kaolin." *Proc. Geotech. Conf.*, Oslo, Norway, 1, 159–163.
24. Zienkiewicz, O. C., and Naylor, D. J. (1972). "The Adaption of Critical State Soil Mechanics Theory for Use in Finite Elements." *Proc. Roscoe Mem. Symp. on Stress-Strain Behavior of Soil*, 537–547.
25. Zienkiewicz, O. C., and Humpheson, C. (1977). "Viscoplasticity—A General Model for Description of Soil Behavior." *Num. Methods Geotech. Engrg.*, Desai and Christian, Eds., McGraw-Hill, New York, N.Y.

APPENDIX IV.—NOTATION

The following symbols are used in this paper:

a = hardening parameter which represents instantaneous size of yield surface;
a_c = size of consolidation surface or pre-yield surface;
B = strength anisotropy factor = M_e/M_c;
$\mathbf{D}$ = elastic stiffness matrix;
$\mathbf{D}^{ep}$ = elastoplastic stiffness matrix;
d = calibration constant defining shape of yield surface on dry side;
$d\epsilon_{ij}$ = total strain increment;
$d\epsilon_{ij}^e$ = elastic strain increment;
$d\epsilon_{ij}^p$ = plastic strain increment;
$d\sigma_{ij}$ = stress increment tensor;
E = Young's modulus;
e_1 = reference void ratio of soil at unit mean stress;
f, F = yield function;
G = shear modulus;
H = hardening modulus;
J_1 = 1st stress invariant;

J_2', J_3' = 2nd and 3rd deviatoric stress invariant;
k = hardening parameter;
M = stress ratio at critical state;
M_c = value of M in case of triaxial compression;
M_e = value of M in case of triaxial extension;
n_{ij} = $n_{ij} = n_{ij}^g = n_{ij}^f$, in case of associated flow rule;
n_{ij}^g, n_{ij}^f = unit normal vector on plastic potential surface and yield surface, respectively;
s = ratio of a/a_c;
α = arbitrary chosen calibration factor;
α_{ij} = tensor which defines translation of yield surface $\alpha_{ij} = (1 - s)\sigma_{ij}^R$;
β, γ = material parameters used in interpolation rule;
δ_{ij} = Kronecker delta;
η = stress ratio (q/p);
θ_0 = Lode angle;
κ_u = initial slope of hydrostatic unloading curve in e-ln p space;
λ_c = slope of hydrostatic loading curve in e-ln p space;
μ = Poisson's ratio;
σ_{ij} = stress tensor;
σ_{ij}^R = stress tensor at point of most recent stress reversal; and
ω = factor defining slope of yield surface at wet side.